Laser and Particle Beams (2015), *33*, 519–524.

doi:10.1017/S0263034615000609

High-intensity terahertz generation by nonlinear frequency-mixing of lasers in plasma with DC magnetic field

ANIL K. MALIK[1,2] AND KUNWAR PAL SINGH[3]

[1]Institute of Optics, University of Rochester, Rochester, New York
[2]Department of Physics, Multani Mal Modi College Modinagar, Chaudhary Charan Singh University Meerut, Uttar Pradesh, India
[3]Singh Simutech Pvt. Ltd., Bharatpur, Rasasthan, India

(Received 16 March 2015; Accepted 13 May 2015)

Abstract

We propose a mechanism of highly focused, tunable and high-intensity terahertz (THz) radiation generation by frequency-mixing of two super-Gaussian lasers with frequencies ω_1, ω_2 and wave numbers k_1, k_2 (laser profile index $p > 2$) in a corrugated plasma in the presence of external static magnetic field $B_0\hat{z}$. In this process, a strong nonlinear ponderomotive force is offered to the plasma electrons at frequency $\omega' = \omega_1 - \omega_2$ and wave number $k' = k_1 - k_2$ by laser beams. The ponderomotive force results in a strong, controllable nonlinear transverse oscillatory current, which can be optimized by optimizing the external magnetic field, ripple parameters, and laser indexes. This controllable current produces focused and intense THz radiation of tunable frequency and power along with a remarkable efficiency ~25%.

Keywords: Plasma; Radiation; Ripples; Terahertz

1. INTRODUCTION

There is growing interest in generating high-intensity and tunable terahertz (THz) radiations to fill the frequency gap ranging from 0.1 to 30 THz due to their enormous applications in chemical and security identification (Shen *et al.*, 2005; Zheng *et al.*, 2006), explosive and concealed weapon detection (Appleby & Wallace, 2007), pharmaceutical quality control and medicine (Zeitler & Gladden, 2008), material characterization, imaging, topography, remote sensing (Ferguson & Zhang, 2002), etc. The increasing availability of high-intensity THz fields is even capable of facilitating the study of nonlinear phenomena (Leinß *et al.*, 2008; Hoffmann *et al.*, 2009; Hirori *et al.*, 2010). Considerable efforts have been made by both the laser community (Köhler *et al.*, 2002; Breunig *et al.*, 2008) and the accelerator community (Krafft, 2004; Byrd *et al.*, 2006; Shen *et al.*, 2007; Neumann *et al.*, 2009) to fill this gap. The use of lasers to generate THz radiation has an advantage of being compact, but it gives limited peak power. The accelerator-based THz sources are capable of providing intense THz radiation with Mega Watt (MW) peak power and are particularly suited for nonlinear optical phenomena and nonlinear spectroscopic measurements (Shen *et al.*, 2007).

Different types of schemes such as THz radiations by super-luminous laser pulse interaction with large band-gap semiconductors and electro-optic crystals (Faure *et al.*, 2004; Jiang *et al.*, 2011) have been proposed to obtain intense and efficient THz sources. The other routes for the THz radiation generation include synchrotron radiation from bunched electrons, transition radiation from electron beams, and THz generations from air plasma filaments (Hamster *et al.*, 1994; Loffler *et al.*, 2000; Carr *et al.*, 2002; Leemans *et al.*, 2003; Dai *et al.*, 2006; Thomson *et al.*, 2007). It has been reported that the efficiency of THz generation can be enhanced if two-color laser pulses are used to create the plasma (Chen *et al.*, 2007). This effect has been attributed to four-wave mixing (Bartel *et al.*, 2005; Thomson *et al.*, 2010) or temporal asymmetries in the *E* fields of the pulses (Wang *et al.*, 2013). Weiss *et al.* (2000) have demonstrated continuous increase in THz power from semiconductors such as GaAs and InAs with increasing magnetic field. Malik *et al.* (2010; 2012) have reported the THz generation in the process of tunnel ionization of a gas jet by femtosecond laser pulses and laser beating in plasmas. A corrugated plasma channel has been proposed for better phase-matched THz radiation generation by the ponderomotive

Address correspondence and reprint requests to: Anil K. Malik, Institute of Optics, University of Rochester, NY 14627, USA. E-mail: anilkmalik@gmail.com

force of a laser pulse (Antonsen *et al.*, 2007; Verma & Sharma, 2009; Varshney *et al.*, 2014). In most of the schemes, the magnetic field has proved to be effective for enhancing the field of emitted radiations (McLaughlin *et al.*, 2000; Weiss *et al.*, 2000; Wu *et al.*, 2007).

It can be observed that most of the THz radiation generation schemes produce either lower average output power (sensitivity) or emit poorly focused radiations. Actually tunable and intense THz radiation with its optimal focusing and collimation has not been realized so far. In the present paper, we show that all these properties can be achieved simultaneously if we generate such radiations through nonlinear frequency-mixing of super-Gaussian (spatial) lasers and employ an external DC magnetic field in a corrugated (density) plasma. Owing to the higher index of the lasers and hence, an enhancement in the steepness in their spatial intensity gradient, a stronger transverse ponderomotive force is realized which drives a very high nonlinear current. This strong, controllable nonlinear oscillatory current is the source for generating THz radiation with tunable frequency, power and focusing properties.

The organization of the paper is as follows. In Section 2, we give analytical results of the electric field and efficiency of the emitted radiation due to nonlinear oscillatory current developed as a result of frequency-mixing of two super-Gaussian lasers of frequencies ω_1, ω_2 and wave numbers k_1, k_2 (profile index $p > 2$). Results and discussion are given in Section 3. Conclusions of the present paper are encapsulated in Section 4.

2. THz RADIATION FIELD AND EFFICIENCY

Figure 1 shows the schematic for the THz generation scheme in the corrugated plasma. We consider frequency-mixing of two super-Gaussian lasers (beam width w_0 and the generalized profile index p) with frequencies ω_1 and ω_2 and wave vectors k_1 and k_2, linearly polarized along the y-direction [pump fields profile $\vec{E}_j = \hat{y}E_{0j}\, e^{(y^{2p}/w_0{}^{2p})}\, e^{i(k_j x - \omega_j t)}$ together with $j = 1, 2$], and co-propagating along the x-direction in a corrugated plasma having density $n = n_0 + n'$ ($n' = n_\alpha e^{i\alpha x}$ together with n_α as the amplitude and α as the wave number of the corrugation) under the effect of magnetic field $B_0\hat{z}$.

The spatial gradient in the laser intensities offers a strong nonlinear ponderomotive force (Malik & Malik, 2013; Malik *et al.*, 2014) to the plasma electrons at frequency $\omega' = \omega_1 - \omega_2$ and wave number $k' = k_1 - k_2$, which is obtained as

$$\begin{aligned}\vec{f}_{\omega'}{}^{\mathrm{NL}} &= -\frac{e^2}{2m_e\omega_1\omega_2}(\nabla\vec{E}_1\cdot\vec{E}_2)^* \\ &= -\frac{e^2E_{01}E_{02}}{2m_e\omega_1\omega_2}\left[\hat{x}ik' - \hat{y}\frac{4py^{2p-1}}{w_0^{2p}}\right] \\ &\quad\times e^{(-(2y^{2p}/w_0{}^{2p}))}e^{i(k'x-\omega' t)},\end{aligned} \tag{1}$$

where m_e is the mass of electron. In the presence of a nonlinear ponderomotive force $\vec{f}_{\omega'}{}^{\mathrm{NL}}$ and the static magnetic field $B_0\hat{z}$, we (Malik *et al.*, 2014) calculate nonlinear density perturbation (say, $n_{\omega'}{}^{\mathrm{NL}}$) using equation of continuity and equation of motion as

$$n_{\omega'}{}^{\mathrm{NL}} = \frac{m_e c^2 n_0}{i\omega'(m_e^2c^2\omega'^2 - e^2B_0^2)}\left[i\omega'\vec{\nabla}\cdot\vec{f}_{\omega'}{}^{\mathrm{NL}} + \vec{\nabla}\cdot\left(\vec{f}_{\omega'}{}^{\mathrm{NL}}\times\frac{eB_0}{m_ec}\hat{z}\right)\right]. \tag{2}$$

This nonlinear density perturbation produces a self-consistent space-charge potential ϕ that leads to a linear density perturbation $n_{\omega'}{}^{\mathrm{L}}$ using which we calculate using Piosson's equation as

$$n_{\omega'}{}^{\mathrm{L}} = \frac{m_e^2c^2\omega_p^2\vec{\nabla}\cdot\left(\vec{\nabla}\phi_{\omega'}\right)}{4\pi e\left(m_e^2c^2\omega'^2 - e^2B_0^2\right)}.$$

Using equation of motion as $m_e\partial\vec{v}_{\omega'}{}^{\mathrm{NL}}/\partial t = \vec{f}_{\omega'}{}^{\mathrm{NL}} + \vec{f}_{\omega'}{}^{\mathrm{L}} - e\left(\vec{v}_{\omega'}{}^{\mathrm{NL}}\times\vec{B}_0\right)$ under the combined effect of $\vec{f}_{\omega'}{}^{\mathrm{NL}}$, $\vec{f}_{\omega'}{}^{\mathrm{L}} = e\vec{\nabla}\phi_{\omega'}$ and magnetic field $B_0\hat{z}$, we calculate the nonlinear velocity of the electrons $\vec{v}_{\omega'}{}^{\mathrm{NL}}$ as

$$\vec{v}_{\omega'}{}^{\mathrm{NL}} = -\frac{e^2E_{01}E_{02}\, e^{(-(2y^{2p}/w_0{}^{2p}))}[T_1\hat{x} + T_2\hat{y}]e^{i(k'x-\omega' t)}}{2m_e^2\omega_1\omega_2(\omega'^2 - \omega_c^2)(\omega'^2 - \omega_H^2)}, \tag{3}$$

where $\omega_c = eB_0/m_ec$,

$$T_1 = \left[\frac{\omega'^2\left(\omega'^2 - \omega_c^2\right) + \omega_c^2\omega_p^2}{c} + \frac{4py^{2p-1}\omega_c\left(\omega'^2 + \omega_p^2 - \omega_c^2\right)}{w_0^{2p}}\right]$$

and

$$T_2 = \left[\frac{i\omega'\omega_c\left(\omega'^2 + \omega_p^2 - \omega_c^2\right)}{c} - \frac{4py^{2p-1}\omega'^2\left(\omega'^2 - \omega_c^2\right) + \omega_c^2\omega_p^2}{i\omega' w_0{}^{2p}}\right],$$

together with $\omega_H = \sqrt{\omega_p^2 + \omega_c^2}$. The nonlinear current $\vec{J}_\omega\left(\equiv -(1/2)n'e\vec{v}_{\omega'}{}^{\mathrm{NL}}\right)$ comprises the contribution from nonlinear perturbations in the electron density $n_{\omega'}{}^{\mathrm{NL}}$ and linear

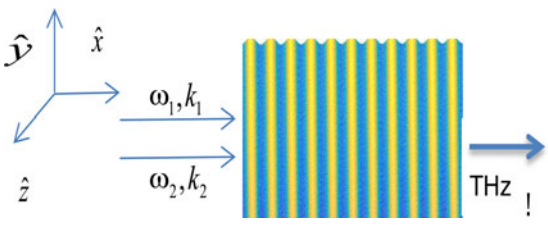

Fig. 1. Schematic representation for the THz generation in the corrugated plasma.

https://doi.org/10.1017/S0263034615000609 Published online by Cambridge University Press

density perturbation $n_{\omega'}{}^{L}$ due to the self-consistent space-charge potential ϕ produced by $n_{\omega'}{}^{NL}$. Hence, the current density $\vec{J}_\omega$ is obtained as

$$\vec{J}_\omega = -\frac{n_\alpha e^3 E_{01} E_{02}}{4m_e^2 \omega_1 \omega_2 (\omega^2 - \omega_c^2)(\omega^2 - \omega_H^2)} e^{-(2y^{2p}/w_0{}^{2p})} \times \{\hat{x}T_1 - i\hat{y}T_2\}\, e^{i(kx-\omega t)}. \tag{4}$$

Here $\omega \equiv \omega' = \omega_1 - \omega_2$ and $\vec{k} = \vec{k}_1 - \vec{k}_2 + \vec{\alpha}$.

We calculate the THz field using Maxwell's equations along with the current $\vec{J}_\omega$ as

$$\vec{\nabla}(\vec{\nabla}\cdot\vec{E}) + \frac{4\pi i\omega}{c^2}\vec{J}_\omega - \frac{\omega^2}{c^2}\bar{\bar{\varepsilon}}\vec{E} - \nabla^2\vec{E} = 0. \tag{5}$$

In the presence of magnetic field, the electric permittivity of the plasma evolves into a tensor quantity $\bar{\bar{\varepsilon}}$ with its components as

$$\varepsilon_{xx} = \varepsilon_{yy} = 1 - \frac{\omega_p^2}{(\omega^2 - \omega_c^2)},$$

$$\varepsilon_{yx} = -\varepsilon_{xy} = \frac{i\omega_c\omega_p^2}{\omega(\omega^2 - \omega_c^2)},$$

$$\varepsilon_{zz} = 1 - \frac{\omega_p^2}{\omega^2},$$

and $\varepsilon_{xz} = \varepsilon_{zx} = \varepsilon_{zy} = \varepsilon_{yz} = 0$. Equation (5) governs the THz radiation emission. Assuming fast phase variation of the field $\vec{E}$, we put $\vec{E} = \vec{E}_0(x, y)\, e^{i(kx-\omega t)}$ in Eq. (5) and separate out the x-and y-components of $\vec{E}$. The normalized transverse component of $\vec{E}$ gives the THz field E_{0y} as

$$\frac{\partial^2 E_{0y}}{\partial x^2} + 2ik\frac{\partial E_{0y}}{\partial x} + \left\{\frac{\omega^2}{c^2}\left(\varepsilon_{yy} + \frac{\varepsilon_{xy}^2}{\varepsilon_{xx}}\right) - k^2\right\}E_{0y} = \left[\left\{\frac{in_\alpha e\omega_p^2 E_{02}\left[\omega^2(\omega^2-\omega_c^2)+\omega_c^2\omega_p^2\right]}{4n_0 m_e c^2\omega_1\omega_2(\omega^2-\omega_H^2)\left[\omega^2-\omega_c^2\right]}\right\}\left[\frac{4py^{p-1}}{w_0{}^p} - \frac{\omega_c\omega_p^2}{c(\omega^2-\omega_H^2)}\right] + \left\{\frac{in_\alpha eE_{02}\omega_c\omega\omega_p^2\left(\omega^2+\omega_p^2-\omega_c^2\right)}{4n_0 m_e c^2\omega_1\omega_2(\omega^2-\omega_H^2)\left[\omega^2-\omega_c^2\right]}\right\}\left[\frac{\omega}{c} - \frac{4py^{p-1}\omega_c\omega_p^2}{w_0{}^p\omega(\omega^2-\omega_H^2)}\right]\right] \times e^{(-2y^{2p}/w_0{}^{2q})} \tag{6}$$

In order to solve Eq. (6), we neglect second-order term and put

$$\left\{\frac{\omega^2}{c^2}\left(\varepsilon_{yy} + \frac{\varepsilon_{xy}^2}{\varepsilon_{xx}}\right) - k^2\right\} = 0.$$

$$\left|\frac{E_{0y}}{E_{01}}\right| = \left|\frac{x}{2k}\left[\left\{\frac{in_\alpha e\omega_p^2 E_{02}\left[\omega^2(\omega^2-\omega_c^2)+\omega_c^2\omega_p^2\right]}{4n_0 m_e c^2\omega_1\omega_2(\omega^2-\omega_H^2)\left[\omega^2-\omega_c^2\right]}\right\}\left[\frac{4py^{p-1}}{w_0{}^p} - \frac{\omega_c\omega_p^2}{c(\omega^2-\omega_H^2)}\right] + \left\{\frac{in_\alpha eE_{02}\omega_c\omega\omega_p^2\left(\omega^2+\omega_p^2-\omega_c^2\right)}{4n_0 m_e c^2\omega_1\omega_2(\omega^2-\omega_H^2)\left[\omega^2-\omega_c^2\right]}\right\}\left[\frac{\omega}{c} - \frac{4py^{p-1}\omega_c\omega_p^2}{w_0{}^p\omega(\omega^2-\omega_H^2)}\right]\right]\right| \times e^{(-2y^{2p}/w_0{}^{2q})}. \tag{7}$$

Here

$$\left\{\frac{\omega^2}{c^2}\left(\varepsilon_{yy} + \frac{\varepsilon_{xy}^2}{\varepsilon_{xx}}\right) - k^2\right\} = 0$$

is a required phase-matching condition for maximum momentum transfer from the lasers to the plasma electrons. From Eq. (7), it is observed that the resonant emission of THz radiations is achieved at $\omega \approx \omega_H \equiv \sqrt{\omega_p^2 + \omega_c^2}$. Since $k_{THz} \neq k'$, a proper tuning of these wave numbers is also required for the resonant excitation of the THz radiation. This tuning is achieved with the help of corrugation (wave number α) in the plasma density (as $\vec{k} = \vec{\alpha} + \vec{k'}$), periodicity (repetition) of which can be obtained from the phase matching condition as

$$|\lambda_{corru}| = \left|\frac{2\pi}{\alpha}\right| = \frac{2\pi c}{\left\{\omega - \sqrt{\frac{\left(\omega^2 - \omega_p^2\right)^2 - \omega^2\omega_c^2}{\omega^2 - \omega_p^2 - \omega_c^2}}\right\}}.$$

The dependence of λ_{corru} on ω_c reveals that the magnetic field plays a vital role in realizing the resonant/phase-matched excitation of the THz radiation at the frequency $\omega \cong \omega_H$ by photo-mixing of the lasers.

Finally, we calculate η_ω as the ratio of average energy densities of the emitted THz radiation to that of the input lasers and that of the emitted THz radiation as follows (Rothwell & Cloud, 2009):

$$\eta_\omega = \frac{px^2 2^{(1/2p)}\mathfrak{R}_1{}^2}{4k^2\Gamma(1/2p)}\left[\frac{8p\mathfrak{R}_2{}^2}{w_0{}^2 2^{(4-1/p)}}\Gamma(2-1/2p) + \frac{\omega^2\mathfrak{R}_3{}^2}{4pc^2 2^{\frac{1}{2p}}}\Gamma(1/2p)\right], \tag{8}$$

where

$$\mathfrak{R}_1 = \frac{n_\alpha e\omega\omega_p^2 E_{02}}{4n_0 mc^2\omega_1\omega_2(\omega^2 - \omega_H^2)\left[\omega^2 - \omega_c^2\right]},$$

$$\mathfrak{R}_2 = \frac{\left[\omega^2(\omega^2 - \omega_c^2) + \omega_c^2\omega_p^2\right]}{\omega} + \frac{\omega_c^2\omega_p^2\left(\omega^2 + \omega_p^2 - \omega_c^2\right)}{\omega\left(\omega^2 - \omega_H^2\right)},$$

https://doi.org/10.1017/S0263034615000609 Published online by Cambridge University Press

and

$$\Re_3 = \frac{\omega_c\omega_p^2\left[\omega^2(\omega^2-\omega_c^2)+\omega_c^2\omega_p^2\right]}{\omega^2\left(\omega^2-\omega_H^2\right)} - \omega_c\left(\omega^2+\omega_p^2-\omega_c^2\right),$$

where Γ is the usual gamma function.

3. RESULTS AND DISCUSSION

The steep corrugations in the density that are constituted at closer distances are suggested for obtaining strong THz radiation (Antonsen *et al*., 2007). Equation (7) shows that the radiation with larger field is obtained for the case of higher amplitude corrugation (higher n_α). This is attributed to the more number of electrons which contribute to excitation of the strong nonlinear current $\vec{J}_\omega$.

Figure 2 shows that the THz amplitude is highest for $\omega/\omega_P \approx 1.3$, that is, near the resonance condition $\omega \approx \omega_H$. Moreover, the role of index (parameter p) of super-Gaussian lasers in getting stronger radiation is evident from the figure, where higher THz field amplitude is obtained for the higher index. Actually for the higher index lasers, a stronger nonlinear current $\vec{J}_\omega$ is realized due to the stronger force $\vec{f}_{\omega'}^{\,NL}$ in the presence of sharp gradient in the lasers' intensity. This gradient is higher in the case of lasers with smaller beamwidth (w_0). Hence, the THz field of higher amplitude is achieved when the lasers of smaller w_0 are used (Fig. 2). A point to be noted in the present scheme is that the THz field $\sim 10^7$ V/cm for the laser intensity $\sim 10^{14}$ W/cm^2 is higher than the field obtained in other schemes (Hamster *et al*., 1994; Loffler *et al*., 2000; Jiang *et al*., 2011; Malik & Malik, 2011; Carr *et al*., 2002; Leemans *et al*., 2003; Dai *et al*., 2006; Chen *et al*., 2007; Thomson *et al*., 2007; Wu *et al*., 2007; 2008; Kim *et al*., 2008).

The most striking feature of the proposed photo-mixing scheme is the tuning of power and focus (transverse profile: y/w_0) of the emitted THz radiation with the help of index of the lasers and magnetic field. In this regard, it is clear from Figure 3 shows that the THz field amplitude attains a maximum value at a particular value of y/w_0. For example, the THz radiation is focused at $y/w_0 = 0.72$ in the case of super-Gaussian lasers of index 2 ($p = 2$), at $y/w_0 = 0.84$ in the case of lasers of index 3 and at $y/w_0 = 0.89$ in the case of lasers of index 4. Moreover, the transverse profile becomes more symmetrical about the y-axis for the case of higher index lasers and peak value of the THz field amplitude is increased with laser index p. The peak field and the collimation of the emitted radiation are further enhanced by increasing magnetic field. The effect of magnetic field becomes more important for the higher index lasers, where we can obtain the radiation of highest intensity at a desired position by changing the index. This is attributed to the higher cyclotron motion of the electrons in the presence of stronger magnetic field.

Equation (8) shows that the present scheme of frequency-mixing of two super-Gaussian lasers is very effective, where the efficiency of about 0.25 can be obtained (Fig. 4) if a combination of the lasers of higher index and a strong magnetic field is used. It can be inferred from the comparison of Figure 4 with Figures 2 and 3 that in the situation of higher efficiency, the THz radiation field is stronger and more focused. This is evident from all the figures that unlike other investigators (Carr *et al*., 2002; Wu *et al*., 2007; 2008; Kim *et al*., 2008), we can get the THz radiation at a desired position along with its tunable power and frequency with the application of an external magnetic field and proper choice of index of the super-Gaussian lasers. Jiang *et al*. (2011) demonstrated a scheme of THz generation scheme based on difference frequency generation by stacking the GaP plates. In their scheme, the conversion efficiency is comparable with our model, but the emitted THz field is much lower than the emitted field in the proposed model. Wu *et al*. reported a scheme of THz generation from the laser wake-field in the inhomogeneous magnetized plasma in which conversion efficiency of the THz radiation is proportional to the laser intensity when it is less than 10^{18} W/cm^2 and it reaches about 10^{-5} when the intensity of the laser is approximately 10^{19} W/cm^2 (Wu *et al*., 2007). Kim

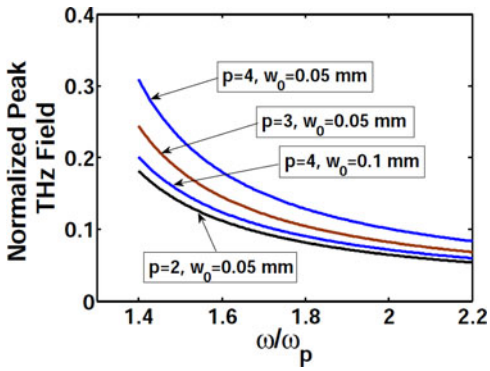

Fig. 2. Variation of the normalized peak THz electric field with index (parameter p) of the lasers and beamwidth (w_0), when $x = 100c/\omega_p$, $\omega_1 = 2.4 \times 10^{14}$ rad/s, $\omega_p = 2 \times 10^{13}$ rad/s, $\omega_c/\omega_p = 0.2$, $n_\alpha/n_0 = 0.2$, $y/w_0 \approx 0.7$, and $|\vec{v}_2^{\,*}| = 0.3c$.

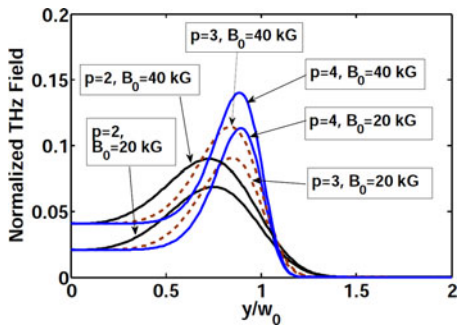

Fig. 3. Transverse profile (y/w_0) of the THz radiation with as a function of magnetic field (B_0) and the index of laser beams, when $w_0 = 0.05$ mm, $x = 100c/\omega_p$, $\omega_1 = 2.4 \times 10^{14}$ rad/s, $\omega_p = 2 \times 10^{13}$ rad/s, $n_\alpha/n_0 = 0.1$, $\omega/\omega_p = 1.45$, and $|\vec{v}_2^{\,*}| = 0.3c$.

https://doi.org/10.1017/S0263034615000609 Published online by Cambridge University Press

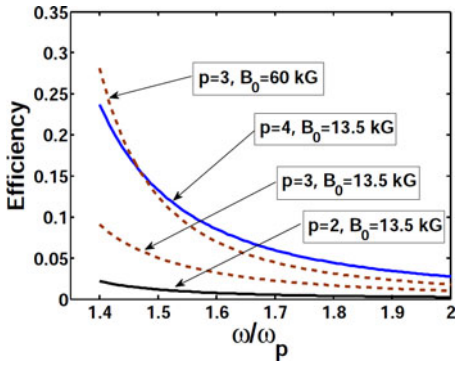

Fig. 4. Efficiency of the THz radiation scheme as a function of magnetic field (B_0) and the index of laser beams for the same parameters as in Fig. 2.

et al. reported generation of THz super-continuum radiation by irradiating different gases with a symmetry-broken laser field composed of the fundamental and second-harmonic laser pulses. The conversion efficiency in their scheme is of the order of ~0.0001 (Kim *et al*., 2008). Hence, it can be seen that the efficiency (say $\eta_\omega = 0.25$) of the present scheme is larger than the previously reported schemes (Wu *et al*., 2007; Kim *et al*., 2008).

4. CONCLUSION

Our analytical calculations show that frequency-mixing of the super-Gaussian lasers in preformed plasma under the effect of magnetic field is a very significant technique for getting efficient THz radiation, where the resonance (phase matching) is easy to achieve by optimizing ripples in the plasma density and the DC magnetic field. The resonance for THz generation is observed at $\omega \cong \omega_H$, which depends on both the plasma frequency and electron cyclotron frequency; therefore resonance frequency $\omega \cong \omega_H$ can shift with the change in magnetic field and hence tuning of the THz frequency from ω_p to $1.8\omega_p$ can be achieved. Since the power depends on resonance condition, it can also be tuned with the help of magnetic field. The magnetic field also helps getting more collimated radiations and enhanced efficiency of the scheme, which can be further increased with proper choice of index of the lasers.

ACKNOWLEDGEMENTS

The author, Anil K. Malik acknowledges UGC support for providing Raman Post Doctoral Fellowship to conduct the research at the Institute of Optics, University of Rochester, Rochester, USA.

REFERENCES

Antonsen, T.M., Palastra, J.J. & Milchberg, H.M. (2007). Excitation of terahertz radiation by laser pulses in nonuniform plasma channels. *Phys. Plasmas* **14**, 033107.

Appleby, R. & Wallace, H.B. (2007). Standoff detection of weapons and contraband in the 100 GHz to 1 THz region. *IEEE Trans. Antennas Propag*. **55**, 2944–2956.

Bartel, T., Gaal, P., Reimann, K., Woerner, M. & Elsacsser, T. (2005). Generation of single-cycle THz transients with high electric-field amplitudes. *Opt. Lett.* **30**, 2805–2807.

Breunig, I., Kiessling, J., Sowade, R., Knabe, B. & Buse, K. (2008). Generation of tunable continuous-wave terahertz radiation by photomixing the signal waves of a dual-crystal optical parametric oscillator. *New J. Phys.* **10**, 073003.

Byrd, J.M., Hao, Z., Martin, M.C., Robin, D.S., Sannibale, F., Schoenlein, R.W., Zholents, A.A. & Zolotorev, M.S. (2006). Tailored terahertz pulses from a laser-modulated electron beam. *Phys. Rev. Lett.* **96**, 164801.

Carr, G.L., Martin, M.C., Mckinney, W.R., Jordan, K., Neil, G.R. & Williams, G.P. (2002). High-power terahertz radiation from relativistic electrons. *Nature* **420**, 153–156.

Chen, Y., Yamaguchi, M., Wang, M. & Zhang, X.C. (2007). Terahertz pulse generation from noble gases. *Appl. Phys. Lett.* **91**, 251116.

Dai, J., Xie, X. & Zhang, X.C. (2006). Detection of broadband terahertz waves with a laser-induced plasma in gases. *Phys. Rev. Lett.* **97**, 103903.

Faure, J., Tilborg, J.V., Kaindl, R.A. & Leemans, W.P. (2004). Modelling laser-based table-top THz sources: Optical rectification, propagation and electro-optic sampling. *Opt. Quantum Electron.* **36**, 681–697.

Ferguson, B. & Zhang, X.C. (2002). Materials for terahertz science and technology. *Nat. Mater.* **1**, 26–33.

Hamster, H., Sullivan, A., Gordon, S. & Falcone, R.W. (1994). Short-pulse terahertz radiation from high-intensity-laser-produced plasmas. *Phys. Rev. E* **49**, 671–677.

Hirori, H., Nagai, M. & Tanaka, K. (2010). Excitonic interactions with intense terahertz pulses in ZnSe/ZnMgSSe multiple quantum wells. *Phys. Rev. B* **81**, 081305.

Hoffmann, M.C., Hebling, J., Hwang, H.Y., Yeh, K.L. & Nelson, K.A. (2009). Impact ionization in InSb probed by terahertz pump-terahertz probe spectroscopy. *Phys. Rev. B* **79**, 161201.

Jiang, Y., Li, D., Ding, Y.J. & Zotova, I.B. (2011). Terahertz generation based on parametric conversion: From saturation of conversion efficiency to back conversion. *Opt. Lett.* **36**, 1608–1610.

Kim, K.Y., Taylor, A.J., Glownia, T.H. & Rodriguez, G. (2008). Coherent control of terahertz supercontinuum generation in ultrafast laser–gas interactions. *Nat. Photonics* **2**, 605–609.

Köhler, R., Tredicucci, A., Beltram, F., Beere, H.E., Linfield, E.H., Davies, A.G., Ritchie, D.A., Iotti, R.C. & Rossi, F. (2002). Terahertz semiconductor-heterostructure laser. *Nature* **417**, 159.

Krafft, G.A. (2004). Compact high-power terahertz radiation source. *Phys. Rev. ST Accel. Beams* **7**, 060704.

Leemans, W.P., Geddes, C.G.R., Faure, J., Tóth, C., Tilborg, J.V., Schroeder, C.B., Esarey, E., Fubiani, G., Auerbach, D., Marcelis, B., Carnahan, M.A., Kaindl, R.A., Byrd, J. & Martin, M.C. (2003). Observation of terahertz emission from a laser–-plasma accelerated electron bunch crossing a plasma-vacuum boundary. *Phys. Rev. Lett.* **91**, 074802.

Leinß, S., Kampfrath, T., Volkmann, K.V., Wolf, M., Steiner, J.T., Kira, M., Koch, S.W., Leitenstorfer, A. & Huber, R. (2008). Terahertz coherent control of optically dark paraexcitons in Cu_2O. *Phys. Rev. Lett.* **101**, 246401.

https://doi.org/10.1017/S0263034615000609 Published online by Cambridge University Press

Loffler, T., Jacob, F. & Roskos, H.G. (2000). Generation of terahertz pulses by photoionization of electrically biased air. *Appl. Phys. Lett.* **77**, 453–455.

Malik, A.K. & Malik, H.K. (2013). Tuning and focusing of terahertz radiation by DC magnetic field in a laser beating process. *IEEE Quantum Electron.* **49**, 232–237.

Malik, A.K., Malik, H.K. & Kawata, S. (2010). Investigations on terahertz radiation generated by two superposed femtosecond laser pulses. *J. Appl. Phys.* **107**, 113105.

Malik, A.K., Malik, H.K. & Stroth, U. (2012). Terahertz radiation generation by beating of two spatial-Gaussian lasers in the presence of a static magnetic field. *Phys. Rev. E* **85**, 016401. [43].

Malik, H.K. & Malik, A.K. (2011). Tunable and collimated terahertz radiation generation by femtosecond laser pulses. *Appl. Phys. Lett.* **99**, 251101.

Malik, H.K., Singh, K.P. & Sajal, V. (2014). Highly focused and efficient terahertz radiation generation by photo-mixing of lasers in plasma in the presence of magnetic field. *Phys. Plasmas* **21**, 073104.

Mclaughlin, R., Corchia, A., Johnston, M.B., Chen, Q., Ciesla, C.M., Arnone, D., Jones, G.A.C., Linfield, E.H., Davies, A.G. & Pepper, M. (2000). Enhanced coherent terahertz emission from indium arsenide in the presence of a magnetic field. *Appl. Phys. Lett.* **76**, 2038–2040.

Neumann, J.G., Fiorito, R.B., O'shea, P.G., Loos, H., Sheehy, B., Shen, Y. & Wu, Z. (2009). Terahertz laser modulation of electron beams. *J. Appl. Phys.* **105**, 053304.

Rothwell, E.J. & Cloud, M.J. (2009). *Electromagnetics*. Boca Raton: CRC Press, 211.

Shen, Y., Watanabe, T., Arena, D.A., Kao, C.C., Murphy, J.B., Tsang, T.Y., Wang, X.J. & Carr, G.L. (2007). Nonlinear Cross-Phase Modulation with Intense Single-Cycle Terahertz Pulses. *Phys. Rev. Lett.* **99**, 043901.

Shen, Y.C., Today, T.W.P.F., Cole, B.E., Tribe, W.R. & Kemp, M.C. (2005). Detection and identification of explosives using terahertz pulsed spectroscopic imaging. *Appl. Phys. Lett.* **86**, 241116.

Thomson, M.D., Blank, V. & Roskos, H.G. (2010). Terahertz white-light pulses from an air plasma photo-induced by incommensurate two-color optical fields. *Opt. Express* **18**, 23173–23182.

Thomson, M.D., Kreß, M., Loffler, T. & Roskos, H.G. (2007). Broadband THz emission from gas plasmas induced by femtosecond optical pulses: From fundaments to applications. *Laser Photonics Rev.* **1**, 349–668.

Varshney, P., Sajal, V., Chauhan, P.K., Kumar, R. & Sharma, N.K. (2014). Effects of transverse static electric field on terahertz radiation generation by beating of two transversely modulated Gaussian laser beams in a plasma. *Laser Part. Beams* **32**, 375–381.

Verma, U. & Sharma, A.K. (2009). Laser second harmonic harmonic generation in a rippled density plasma in the presence of azimuthal magnetic field. *Laser Part. Beams* **27**, 719–724.

Wang, W.M., Li, Y.T., Sheng, Z.M., Lu, X. & Zhang, J. (2013). Terahertz radiation by two-color lasers due to the field ionization of gases. *Phys. Rev. E* **87**, 033108.

Weiss, C., Wallenstein, R. & Beigang, R. (2000). Magnetic-field-enhanced generation of terahertz radiation in semiconductor surfaces. *Appl. Phys. Lett.* **77**, 4160–4162.

Wu, H.C., Sheng, Z.M., Dong, Q.L., Xu, H. & Zhang, J. (2007). Powerful terahertz emission from laser wakefields in inhomogeneous magnetized plasmas. *Phys. Rev. E* **75**, 016407.

Wu, H.C., Sheng, Z.M. & Zhang, J. (2008). Single-cycle powerful megawatt to gigawatt terahertz pulse radiated from a wavelength-scale plasma oscillator. *Phys. Rev. E* **77**, 046405.

Zeitler, J.A. & Gladden, L.F. (2008). n-vitro tomography and non-destructive imaging at depth of pharmaceutical solid dosage forms. *Eur. J. Pharm. Biopharm.* **71**, 2–22.

Zheng, H., Sanchez, A.R. & Zhang, X.C. (2006). Identification and classification of chemicals using terahertz reflective spectroscopic focal plane imaging system. *Opt. Express* **14**, 9130–9141.

https://doi.org/10.1017/S0263034615000609 Published online by Cambridge University Press